J. Phycol. **57,** 435–446 (2021)

DOI: 10.1111/jpy.13125-20-132

NO EVIDENCE OF PHAGO-MIXOTROPY IN *MICROMONAS POLARIS* (MAMIELLOPHYCEAE), THE DOMINANT PICOPHYTOPLANKTON SPECIES IN THE ARCTIC[1]

Valeria Jimenez

Ecology of Marine Plankton, Sorbonne Université, CNRS, UMR7144, Station Biologique de Roscoff, Roscoff 29680, France

John A. Burns

Bigelow Laboratory for Ocean Sciences, East Boothbay, ME,USA

Florence Le Gall, Fabrice Not

Ecology of Marine Plankton, Sorbonne Université, CNRS, UMR7144, Station Biologique de Roscoff, Roscoff 29680, France

and Daniel Vaulot[2]

Ecology of Marine Plankton, Sorbonne Université, CNRS, UMR7144, Station Biologique de Roscoff, Roscoff 29680, France
Asian School of the Environment, Nanyang Technological University, 50 Nanyang Avenue, Singapore 639798, Singapore

In the Arctic Ocean, the small green alga *Micromonas polaris* dominates picophytoplankton during the summer months but is also present in winter. It has been previously hypothesized to be phago-mixotrophic (capable of bacteria ingestion) based on laboratory and field experiments. Prey uptake was analyzed in several *M. polaris* strains isolated from different regions and depths of the Arctic Ocean and in *Ochromonas triangulata*, a known phago-mixotroph used as a control. Measuring ingestion of either fluorescent beads or fluorescently labeled bacteria by flow cytometry, we found no evidence of phago-mixotrophy in any *M. polaris* strain while *O. triangulata* was ingesting both beads and bacteria. In addition, *in silico* predictions revealed that members of the genus *Micromonas* lack a genetic signature of phagocytotic capacity.

Key index words: **Arctic; *Micromonas*; phago-mixotrophy; phytoplankton**

***Abbreviations*: ASW, Artificial seawater; L1-ASW, L1 medium prepared with artificial seawater; YG-beads, Yellow-green fluorescent polystyrene-based microsphere; FLBs, Fluorescently labeled bacteria; FALS, Forward Angle light scatter; EXP, Experiment; Ab, Addition of antibiotics (penicillin–streptomycin–neomycin, PSN)**

Polar regions are undergoing drastic changes due to climate change and global warming in particular. These changes have strong effects in Arctic marine ecosystems (Graversen et al. 2008, Wassmann 2015, Box et al. 2019) where phytoplankton production plays an essential role in food web dynamics and biogeochemical cycles (Arrigo et al. 2008, Park et al. 2015, Kahru et al. 2016). Considerable spatial and temporal changes in primary production have been observed in the last two decades (Kahru et al. 2016, Renaut et al. 2018, Tedesco et al. 2019). Rapid melting and early ice retreat increase the open areas exposed to solar radiation which in turns could result in an increase in annual net primary production along with a lengthening of the phytoplankton growing season (Park et al. 2015, Kahru et al. 2016, Renaut et al. 2018). Changes in Arctic primary production are also influenced by the increase of freshwater delivery to the upper ocean that leads to stronger water column stratification limiting the upward flux of nutrients to the surface (Timmermans et al. 2011, Coupel et al. 2015, Park et al. 2015, Slagstad et al. 2015, Tremblay et al. 2015, Nummelin et al. 2016, Brown et al. 2019).

Our ability to explain and predict the responses of Arctic phytoplankton communities to climate change is challenged by our limited understanding regarding their ecological and physiological strategies of growth and survival. Arctic phytoplankton communities experience extreme environmental conditions such as nutrient limitation, exposure to a long period of darkness (polar winter) followed by low light levels under the ice linked to snow coverage and ice thickness (Berge et al. 2015). In such unfavorable and shifting context, it has been suggested that phago-mixotrophy (ability to combine photosynthesis and bacterivory) could be a common trophic strategy among Arctic protists (Stoecker and Lavrentyev 2018). At the scale of the global ocean, phago-mixotrophy is an important, but until recently underestimated, process for energy and

[1]Received 8 June 2020. Revised 28 November 2020. Accepted 6 December 2020.
[2]Author for correspondence: e-mail vaulot@gmail.com
Editorial Responsibility: M. Herron (Associate Editor)

nutrient transfer (e.g., carbon fluxes) throughout the food web (Mitra et al. 2014, Caron 2016, Ward and Follows 2016). Phago-mixotrophic plankton are widespread in the ocean and evolutionary diverse, found in many branches of the eukaryotic tree (Selosse et al. 2017). They account for a large proportion of bacterivory in aquatic environments (Hartmann et al. 2012, Unrein et al. 2014, Leles et al. 2019). A recent study (Stoecker and Lavrentyev 2018) reviews the current evidence and importance of phago-mixotrophy in the Arctic ocean where this trophic mode has been documented in chrysophytes (e.g., *Ochromonas* spp., *Dinobryon balticum*), cryptophytes (e.g., *Geminigera cryophila*, *Teleaulax amphioxeia*), prymnesiophytes (e.g., *Chrysochromulina* spp.), dinoflagellates (e.g., *Heterocapsa triquetra*, *Tripos arcticus*), and chlorophytes (e.g., *Pyramimonas* spp.).

The ongoing expansion of stratification and nutrient limitation in the Arctic have been associated with an observed increase of the smaller picophytoplankton (Li et al. 2009, Ward 2015) which ranges from 2 to 3 μm in cell diameter and is composed essentially of eukaryotes since cyanobacteria are nearly absent in polar marine ecosystems (Paulsen et al. 2016). Among the picoeukaryotic phytoplankton community, the green alga *Micromonas polaris* (Lovejoy et al. 2007, Simon et al. 2017) dominates in the Arctic ocean in the summer months (Lovejoy et al. 2007, Balzano et al. 2012, Kilias et al. 2014, Marquardt et al. 2016) but is also present throughout the winter (Joli et al. 2017). Its abundance is expected to increase as the stratified oligotrophic areas expand (Li et al. 2009, Hoppe et al. 2018, Benner et al. 2020). The physiological plasticity allowing *M. polaris* to dominate the Arctic picoeukaryote community is not yet well understood. *M. polaris* was shown in the laboratory, to positively respond to a combination of temperature increase and acidification by higher growth rate and biomass production (Hoppe et al. 2018). Phago-mixotrophy would be another advantageous trait that could contribute to the success of *M. polaris* in the Arctic. Under prolonged periods of darkness or low irradiance, phago-mixotrophs could survive, despite reduced or even null rates of photosynthesis, by supplementing their carbon requirements through phagocytosis (Zhang et al. 1998, Millette et al. 2017, Stoecker and Lavrentyev 2018). Under oligotrophic conditions, phago-mixotrophy could also supply the cell with limiting nutrients (Stoecker et al. 2017).

Evidence of phago-mixotrophy in *Micromonas* has been previously obtained in laboratory and field experiments (Gonzalez et al. 1993, Sanders and Gast 2012, McKie-Krisberg and Sanders 2014, McKie-Krisberg et al. 2018). More than 25 years ago, Gonzalez et al. (1993) reported phago-mixotrophy in a temperate *Micromonas* strain (identified at that time as *M. pusilla*) based on a positive acid lysozyme assay and ingestion of fluorescently labeled bacteria (FLBs) measured by microscopy. More recently, the ability of Arctic pico and nanoplankton microbial communities to consume bacterioplankton has been analyzed by in situ experiments using FLBs and yellow-green fluorescent microspheres (YG-beads) as prey. A *Micromonas*-like picoeukaryote, based on its shape and analysis of denaturing gradient gel electrophoresis (DGGE) band sequences, was reported to ingest a significant quantity of prey offered to it (Sanders and Gast 2012). Ingestion of beads was further tested in *M. polaris* strain CCMP2099 under laboratory conditions that compared different light levels and nutrient concentrations. The highest grazing rates were observed under light and low nutrient conditions (McKie-Krisberg and Sanders 2014) for which transcriptional response was also investigated (McKie-Krisberg et al. 2018). Despite the evidence presented, it is still unclear whether *M. polaris* is capable of ingesting bacteria because of the difficulty to distinguish whether the prey are inside the cells or just externally attached to them (Wilken et al. 2019) when using epifluorescence microscopy. Recently, association of YG-beads with *M. polaris* (strain CCMP2099) cells was found after performing feeding experiments with heat-killed cultures (Wilken et al. 2019), suggesting that beads may stick to the surface of the cells resulting in a potential over-estimation of phagocytosis.

In the present paper, we used flow cytometry to analyze prey uptake in several *Micromonas polaris* strains isolated from different regions and depths in the Arctic Ocean (including the CCMP2099 strain previously reported as mixotrophic by McKie-Krisberg and Sanders 2014) and used the chrysophyte *Ochromonas triangulata*, which is a phago-mixotroph (Andersen et al. 2017), as a positive control. We also made predictions of the capacity of *Micromonas* to be a phago-mixotroph from an in silico gene-based model.

MATERIALS AND METHODS

Strains and culturing conditions. Four *Micromonas polaris* strains and one phago-mixotrophic *Ochromonas triangulata* strain were used in this study. Three of the *M. polaris* strains (RCC2306, RCC4298, and RCC2258) and *O. triangulata* strain RCC21 (previously known as *O. distigma*, Andersen et al. 2017) were obtained from the Roscoff Culture Collection (RCC, http://www.roscoff-culture-collection.org). The fourth *M. polaris* strain (CCMP2099) was obtained from the Provasoli-Guillard National Center for Culture of Marine Phytoplankton and Microbiota (https://ncma.bigelow.org) and is also available from the RCC as RCC807. The *M. polaris* strains originate from different locations and depths in the Arctic (Table 1). All strains were nonaxenic and grown under a 12:12 h light:dark cycle at 80 μmol photons $\cdot$ m^{-2} $\cdot$ s^{-1} PAR using L1 medium (Guillard and Hargraves 1993) made with artificial seawater (ASW, salinity 35; Keller et al. 1987). All *M. polaris* strains were grown at 4°C and *O. triangulata* at 20°C. Cells were acclimated and maintained in mid-exponential growth phase before the beginning of each experiment.

Cell monitoring, feeding estimates and sample fixation. Cells and prey were counted using a Guava easyCyte (Luminex Corporation, Austin, TX, USA) flow cytometer (FCM) equipped with a 488 nm laser recording cell counts, forward and side angle light scatters (FALS and SSC), both proxies of cell size, green (525 ± 30 nm band pass filter) and red (695 ± 50 nm band pass filter) fluorescences. Cultures under the different experimental conditions were monitored live using red autofluorescence from chlorophyll as a threshold. Flow cytometry was also used to determine the percent of cells with prey (YG-beads and FLBs) in samples fixed using a protocol modified from Sherr and Sherr (1993) (acid Lugol's iodine solution and formaldehyde 3.7%, and cleared with sodium thiosulfate 3%) with a threshold either on red fluorescence or green fluorescence. With the threshold on red fluorescence, cells that contained chlorophyll as well as green fluorescence (same signal as the prey added: YG-beads or FLBs) were considered to be cells containing prey (Fig. S1 in the Supporting Information). In addition, to confirm the total concentration of prey added to each flask, the sample was also run with the threshold on green fluorescence. FCM list modes were analyzed with the Guava easyCyte Suite Software 3.1 (Luminex Corporation).

For each feeding experiment, the ingestion of prey was quantified in each experimental flask by first adding prey and then sub-sampling and fixing after an incubation of 0 (T_0), 20 (T_{20}), and 40 (T_{40}) min. The T_0 sample accounts for the physical attachment of prey to the cell and therefore the percent of cells ingesting prey corresponds to the percent of cells with prey at T_{20} or T_{40}, minus the percent of cells with prey at T_0.

Microscopy. Light limited *Micromonas polaris* (strain RCC2306) cells were fixed just after the addition of YG-beads (T_0) with glutaraldehyde (1% final concentration). Fixed cells were sedimented onto formvar coated copper grids for 30 min. Grids were then stained with three drops of uranyl acetate 2%, dried, and examined using a JEOL JEM1400 transmission electron microscopy (TEM, Jeol, Tokyo, Japan) operating at 80 kV. Images were obtained with a Gatan Orius camera (Roper Scientific SAS, France).

Major feeding experiments. To test feeding, three different experimental designs were performed with *Micromonas polaris* strains and another fourth with *Ochromonas triangulata* (Table 2). Feeding was primarily tested using yellow-green fluorescent polystyrene-based microspheres (YG-beads, diameter 0.5 μm, Fluoresbrite, Polysciences, Inc., Warrington, PA, USA) as prey. In some experiments, fluorescently labeled bacteria (FLBs) were used. FLBs were prepared according to the protocol of Sherr et al. (1987) using the bacteria *Brevundimonas diminuta* (strain CECT313, also named *Pseudomonas diminuta*), obtained from the Spanish Type Culture Collection (CECT, Valencia, Spain).

In experiment type 1 (*Micromonas polaris*-EXP1), feeding was tested for each *M. polaris* strain grown under four different culture conditions. Each treatment was carried out (in duplicates for RCC2306 and RCC4298 and triplicates for RCC2258 and CCMP2099) by transferring a small volume of culture (a few mL in general), previously maintained in mid-exponential growth, to about 40 mL of L1-ASW medium (replete) or ASW without any addition (limited) in a 50-mL culture flask and then placed in the dark or left in the same light conditions as for culture maintenance. Each treatment (light replete, light limited, dark replete, and dark limited) was followed up for 15-17 d and feeding was tested with YG-beads after 7 (Feeding 1) and 14-17 (Feeding 2) d.

Experiment type 2 (*Micromonas polaris*-EXP2) was performed with *M. polaris* strain RCC2306 and RCC2258 and was set-up the same way as EXP1 (in triplicates), but with an additional treatment (light replete-Ab) in which 1 μL of penicillin–streptomycin–neomycin (PSN) antibiotics solution (Sigma-Aldrich P4083) was added per mL of culture at the beginning of the experiment in order to minimize bacteria concentration. Moreover, the five treatments were incubated for only one week and feeding was tested with YG-beads at the end of the incubation (Day 7).

To compare feeding on YG-beads vs. FLBs, a third type of experiment (*Micromonas polaris*-EXP3) was performed with *M. polaris* RCC4298. For each prey type (YG-beads and FLBs) feeding was tested in triplicate in mid-exponential phase cultures (light replete).

For all experiments (*Micromonas polaris*-EXP1 to EXP3), the initial concentration for each treatment was 5×10^5 cells · mL^{-1}. The prey concentration was adjusted as a function of the actual cell concentration at the time of the feeding experiment in order to achieve a prey to cell ratio of 1.5 to 2.5. As a consequence, prey concentration varied between 3×10^3 and 50×10^6 beads · mL^{-1}.

The experimental design of experiments EXP1 and 2 performed with *Ochromonas triangulata* was the same and only differed in their replication and number of feeding time points. *O. triangulata*-EXP1 was conducted in duplicate and with three feeding time points (T_0, T_{20}, and T_{40}), and *O. triangulata*-EXP2 in triplicates and two feeding time points (T_0 and T_{40}). Feeding was tested under two different culture conditions by transferring a small volume of culture, previously maintained in mid-exponential growth, to L1-ASW medium (light replete) or ASW without any addition (light limited) and incubated in the same light conditions as for culture maintenance. After one week of incubation, feeding was tested with YG-beads. The third experiment type (*O. triangulata*-EXP3) was performed in parallel with *Micromonas polaris*-EXP3 to compare feeding on YG-beads and FLBs. For each prey type (YG-beads and FLBs), feeding was tested in biological triplicates in mid-exponential phase cultures (light replete). In a fourth experiment type (*O. triangulata*-EXP4), feeding was tested using FLBs as prey in light replete culture conditions. EXP4 was performed two times (EXP4a and b) and each time in duplicates.

Additional experiments. The degree of attachment of YG-beads to cells, immediately after the addition of prey (T_0) was further examined in a number of additional experiments (*M. polaris*-EXP5) performed with *Micromonas polaris* strains

TABLE 1. List of algal strains used in this study with isolation region, coordinates, depth (m), and growth temperature (°C).

Species	Strain	Origin	Lat, Long	Depth	Temperature
Micromonas polaris	CCMP2099	Arctic, Baffin Bay	76° N, 75° W	55	4
	RCC2306	Arctic, Beaufort Sea	71° N, 132° W	70	4
	RCC4298	Arctic, Greenland Sea	82° N, 20° E	20	4
	RCC2288	Arctic, Beaufort Sea	70° N, 135° W	0	4
Ochromonas triangulata	RCC21	Atlantic, Bay of Biscay	48° N, 4° W	-	20

TABLE 2. Experimental scheme. Replete corresponds to cultures grown in artificial seawater (ASW) with L1 medium components added and limited to cultures grown in ASW without any addition. Ab correspond to cultures for which 1 µL of penicillin–streptomycin–neomycin (PSN) antibiotics solution was added to 1 mL of culture. The time points on which the percent of cells with prey was measured is indicated (T_0, T_{20}, and T_{40}, where the subscript corresponds to min). LR: Light nutrient replete, LL: Light nutrient limited, DR: Dark nutrient replete, DL: Dark nutrient limited, LR-Ab: Light nutrient replete with antibiotics.

Code	Conditions	Prey	Genus	Time points (min)	Goal
EXP1	LR, LL, DR, DL	YG-beads	*Micromonas*, *Ochromonas*	0, 20, 40	Basic experiment with beads
EXP2	LR, LL, DR, DL, LR-Ab	YG-beads	*Micromonas*, *Ochromonas*	0, 20, 40	Test effect of antibiotics
EXP3	LR	YG-beads, FLBs	*Micromonas*, *Ochromonas*	0, 40	Compare beads vs. FLBs
EXP4	LR	FLBs	*Ochromonas*	0, 40	Test FLBs on *Ochromonas*
EXP5	LR, LL, DR, DL, LR-Ab	YG-beads	*Micromonas*	0	Test attachment of preys at T_0
EXP6	LR	YG-beads	*Micromonas*	0, 40	Test effect of fixation
EXP7	LL	YG-beads	*Micromonas*	0, 40	Test effect of bead size
EXP8	LR	YG-beads	*Micromonas*	0 to 20	Time course of bead attachment
EXP9	LL	YG-beads	*Micromonas*, *Ochromonas*		Test Lysosensor (food vacuoles)

RCC2306 and RCC4298. For *M. polaris* strain RCC2306, the quantification was done in cultures grown under light replete, light limited, dark replete, and dark limited conditions, and for *M. polaris* strain RCC4298 with cultures grown under these four conditions plus light replete-Ab.

The effects of fixation on the attachment of YG-beads to cells (*Micromonas polaris*-EXP6) was measured by simultaneously comparing feeding in experiments performed with *M. polaris* (strain RCC2306) and run in the flow cytometer live or after fixation with Lugol's iodine solution and glutaraldehyde (0.25% final concentration). For this experiment, *M. polaris* (strain RCC2306) in mid-exponential (light replete) feeding was measured at two time points (T_0 and T_{40}).

Feeding on three different YG-bead sizes (0.5, 1, and 2 µm in diameter; *Micromonas polaris*-EXP7) was measured in *M. polaris* (strain RCC2306) incubated for one week in light limited conditions (duplicates). Feeding was measured independently for each bead size using two feeding time points (T_0 and T_{40}).

Changes in the number of cells with YG-beads were measured by continuously running a live sample for 20 min immediately after the addition of YG-beads (*Micromonas polaris*-EXP8). Samples were quantified on the FACSCanto (BD Biosciences, San Jose, CA, USA) flow cytometer with the same configuration as the Guava. For this experiment, cultures of *M. polaris* (strain RCC2306), previously incubated for one week in light limited conditions, were used. Two ratios of beads to cells were tested (ratio of 1:1 and 2:1) in duplicates.

The percent of cells potentially containing food vacuoles (EXP9) was quantified in *Micromonas polaris* (strain RCC2306) and *Ochromonas triangulata*, stained with the probe LysoSensor Green DND-189 (Thermo Fisher Scientific, Waltham, MA, USA), that accumulates in acid cellular compartments like food vacuoles, at a final concentration of 1 µM. After the addition of LysoSensor, cells were incubated in the dark for 8 min and measured for 2 min using the Guava easyCyte (Luminex Corporation) flow cytometer (triggered on green fluorescence). Cells with higher green fluorescence, after incubation with LysoSensor, were considered as potentially containing food vacuoles (Fig. S2 in the Supporting Information). The cells used for this test came from light limited cultures (duplicates), from *O. triangulata*-EXP1 and *M. polaris*-EXP2, on which feeding experiments were performed.

Data analysis. Data processing, graphics, and statistical analyses were performed using the R software (R Core Team 2014) using in particular the package set *tidyverse*. Pairwise comparisons were performed with the *t.test* function to calculate *p*-values based on Student (assuming equal variances) and Welch (assuming unequal variances) t-test.

Trophic mode predictions from genome and transcriptome analysis. Predicted peptides from whole genome (Worden et al. 2009, van Baren et al. 2016) or transcriptome data (Keeling et al. 2014) were downloaded from publicly available databases as detailed in Table S1 in the Supporting Information. Because computational predictions are based on presence/absence information, predicted peptides from independent transcriptome assemblies of the same strain were concatenated to include as much information about each strain as possible. Computational prediction of phagocytotic, photosynthetic, and prototrophic capabilities was completed as in Burns et al. (2018). This involved scoring a set of 14,095 protein profile hidden Markov models (HMMs) that were derived by clustering all proteins in 35 reference eukaryote genomes of known trophic mode against all proteins from each test genome or transcriptome. HMM profiles with a full sequence e-value $\leq 10^{-5}$ and a single domain e-value $\leq 10^{-4}$ to any protein in a test genome or transcriptome were marked as "present" for that organism. Predictive models of trophic modes were built by grouping the reference eukaryotes by known trophic mode and discovering HMMs from the set of 14,095 proteins that had differential presence/absence patterns between groups. Those HMMs whose presence/absence patterns differed according to trophic mode were annotated against Swiss-Prot and grouped by gene ontology (GO) terms. GO categories were scored per reference organism, and a best predictive set of GO terms was selected for each trophic mode using machine learning algorithms, forming the core of the predictive trophic mode models. Each test genome/transcriptome was scored for the predictive GO categories of the trophic mode models using its HMM presence/absence vector. Final prediction probabilities for each test genome/transcriptome were calculated against the reference trophic mode models using a probability neural network. To visualize the prediction output, which exists in four dimensions with three degrees of freedom (phagocytosis, photosynthesis, prototrophy, and a fourth dependent dimension for absence of each trophic mode), predictions were normalized such that the sum of the three predictions plus the probability of not fitting each trophic mode equaled 1 using the relation: $1-(p_{phago} + p_{proto} + p_{photo})/3$. The fractional independent probabilities of each trophic mode and the dependent absence number were mapped to 4-dimensional color space and projected onto a circle using scripts adapted from the R package *pavo* (Maia et al. 2013). Scripts are available at https://github.com/burnsajohn/predictTrophicMode.

RESULTS

Feeding experiments. *Micromonas polaris* feeding was analyzed in four strains (CCMP2099, RCC2306, RCC4298, and RCC2258; Table 1) using a slight modification of the protocol described in Sherr and Sherr (1993). We determined the percentage of cells feeding on YG-beads or FLBs using flow cytometry to quantify the proportion of cells with prey. Compared to epifluorescence microscopy, which is low throughput allowing examination of at most 100 to 200 cells per sample (e.g., McKie-Krisberg and Sanders 2014), flow cytometry allows screening of a large number of cells per sample (typically several thousand). It also circumvents ambiguities that arise with microscopy when cells and prey randomly overlap during the filtration process (Wilken et al. 2019). To validate our approach, we used the phago-mixotrophic *Ochromonas triangulata* strain RCC21 as a positive control. A range of experiments were performed to test different parameter combinations (Table 2).

Micromonas polaris strains were grown under a combination of 2 light regimes and 2 nutrient concentrations (*M. polaris*-EXP1: light nutrient replete, light nutrient limited, dark nutrient replete, and dark nutrient limited). Experiments took place over a period of 15 to 17 d. Feeding was examined with YG-beads after 7 (Feeding 1) and 14-17 d (Feeding 2). Clear negative growth effects under darkness and nutrient limitation conditions were observed for all strains. Overall, for all 4 strains under dark conditions, growth ceased between day 4 and day 7, and thereafter, cell concentration remained stable (Fig. 1). For cultures grown under low nutrient conditions in the light (light limited), a decrease in growth rate was observed after one week (Fig. 1). Additional signs of the effect of darkness and nutrient limitation were observed in FALS (proxy of cell size) and chlorophyll fluorescence: For example, FALS decreased for cells in the dark (Fig. S3 in the Supporting Information). In all feeding experiments, we observed that cells at time T_0, immediately following addition of the beads, already had a number of beads associated with them. However, no significant difference was observed between the percent of cells with YG-beads at T_0 vs. T_{20} or T_{40} whatever the growth phase or the culture condition (Figs. 2A and S4, Table S2 in the Supporting Information).

We questioned whether the absence of feeding on YG-beads could have been due to the presence of bacteria in the cultures. In order to address this issue, we performed a second series of experiments in which we included a fifth condition by adding antibiotics to a light nutrient replete culture (*Micromonas polaris*-EXP2). This was only performed with two of the *M. polaris* strains (RCC2258 and RCC2306), and a single feeding experiment was conducted after one week. No feeding was detected under any of the culture conditions (Fig. S5 in the Supporting Information).

We then compared feeding on YG-beads vs. FLBs as prey (*Micromonas polaris*-EXP3) since the prey type may influence feeding behavior. Again no feeding was observed when using either YG-beads or FLBs (Fig. 2B). In contrast, in the four experiments performed with *Ochromonas triangulata* (EXP1 to EXP4) we observed feeding on YG-beads and FLBs that ranged from 7 to 14 and 21 to 27 percent of cells feeding on each prey type respectively, suggesting that *Ochromonas* clearly preferred FLBs over YG-beads (Fig. 2B, Table S2).

The percentage of cells with 0.5 μm YG-beads at T_0 was linearly related to bead concentration (Fig. 3, $R^2 = 0.93$). Cell size did not seem to have an influence since *Micromonas* (~ 1.5 μm) and *Ochromonas* (~ 5 μm) fitted the same curve (Fig. 3). The number of cells with YG-beads did not change over time as demonstrated by monitoring live cells of *M. polaris* (strain RCC2306) in the presence of YG-beads by flow cytometry over a 20-minute period (Fig. S6 in the Supporting Information).

The association of beads and cells did not seem to be linked to bead size. We still observed association of 1 and 2 μm YG-beads with cells at T_0, even though the 2 μm beads are close in size to *Micromonas polaris* cells and no differences were observed between the percent of cells with YG-beads at T_0 and T_{40} (Fig. S7 and Table S3 in the Supporting Information). Fixation does not seem to impact the association of beads at T_0 as we observed this co-association when samples were run live or fixed with Lugol's solution or glutaraldehyde (Table S4 in the Supporting Information). External attachment of YG-beads to cells of *M. polaris* (strain RCC2306) was visualized by TEM (Fig. S8 in the Supporting Information).

Since the observation of acidic food vacuoles has been proposed as evidence of phagotrophy (Carvalho and Graneli 2006, Wilken et al. 2019), light nutrient limited cultures of *Micromonas polaris* (from EXP-2, which did not feed on YG-beads) were stained with the acidotropic LysoSensor fluorescent probe. No significant difference was observed in green LysoSensor fluorescence between unstained and stained cells, whereas for *Ochromonas triangulata* (EXP1 light nutrient limited) green fluorescence increased 3.5 times after staining, suggesting the presence of food vacuoles in the latter species (Fig. S2 and Table S5 in the Supporting Information).

Trophic mode predictions. Phagocytotic, photosynthetic, and prototrophic capacity of protists can be predicted based on their genome or transcriptome composition (Burns et al. 2018). We used this approach to analyze gene composition of a number of microalgae including *Micromonas* (Table S1). The predictions confirm that known phago-mixotrophs like *Dinobryon* sp., Pedinelalles sp., *Ochromonas triangulata*, and *Prymnesium parvum* have and express a

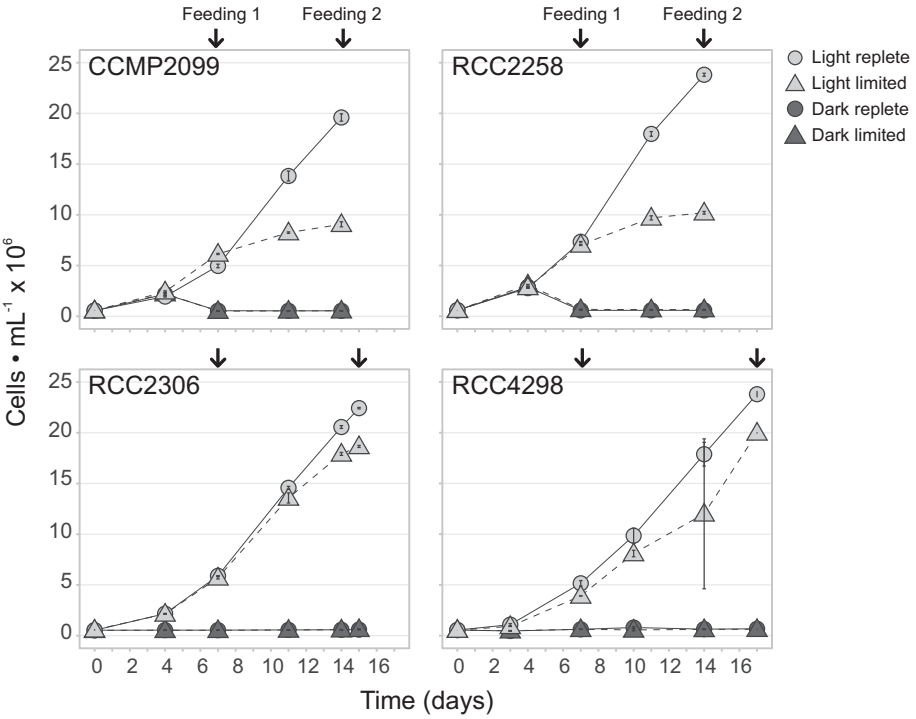

FIG. 1. Growth curves for each *Micromonas polaris* strain grown under four treatments (*M. polaris*-EXP1). Arrows indicate the time point (d) when a feeding experiment was performed. Error bars correspond to standard deviation and in some cases are smaller than the symbol used.

battery of genes consistent with their observed lifestyle coherent with the capacity for phagocytosis, photosynthesis, and prototrophy (Fig. 4). Presumed photo-autotroph like members of the genus *Ostreococcus* lack genes consistent with the capacity for phagocytosis, but have genes consistent with the capacity for photosynthesis and prototrophy (Fig. 4). Similarly, all members of the genus *Micromonas* are predicted to be photo-autotroph as they contain genes consistent with photosynthesis and prototrophy, but lack genes consistent with the capacity for phagocytosis (Fig. 4).

DISCUSSION

We examined feeding of *Micromonas polaris* in a series of experiments with four different strains (CCMP2099, RCC2306, RCC4298, and RCC2258) grown under different light and nutrient conditions using flow cytometry to monitor prey uptake (Table 2). Significant differences were not detected between the number of *M. polaris* cells associated with prey at T_0 and other time points (T_{20} or T_{40}) in any of these experiments (Figs 2, S4 and S5, Table S2). We also tested different fixation methods vs. live cells and three different diameters of beads (0.5, 1, and 2 μm in diameter) without detecting any suggestion of active uptake by *M. polaris*. No evidence of phago-mixotrophy was found when using the acidotropic LysoSensor dye in *M. polaris* light nutrient limited cultures. Trait-based computational analysis of available genomes and transcriptomes confirmed that *Micromonas* lack genes consistent with the capacity for phagocytosis. These data are in contrast to what was observed for the known phagotroph *Ostreococcus triangulata* (strain RCC21) that always displayed evidence of prey uptake when using similar approaches to the one we used for *M. polaris* strains and fits the computational profile of a phago-mixotroph. None of our evidence is consistent with the consideration of *M. polaris* as a phago-mixotroph.

In each of our experiments, there was a considerable number of *Micromonas polaris* cells at T_0 associated with prey, immediately following addition of prey to the cultures and before time had elapsed for prey ingestion. The percentage of cells with 0.5 μm YG-beads at T_0 appears to be linearly related to the bead concentration (Fig. 3), suggesting the association is the result of a physical property of the cell's surface rather than an active behavior that the cells execute. The external attachment of YG-beads to *M. polaris* cells was also visualized by electron microscopy (Fig. S8). Such passive associations of cells with beads have recently been observed in *Micromonas* by Wilken et al. (2019) using flow cytometry. They observed that the proportion of cells associated with beads at T_0 was much larger for heat-killed vs. live cells and that in live cells it increased with time for cultures left in the dark compared to

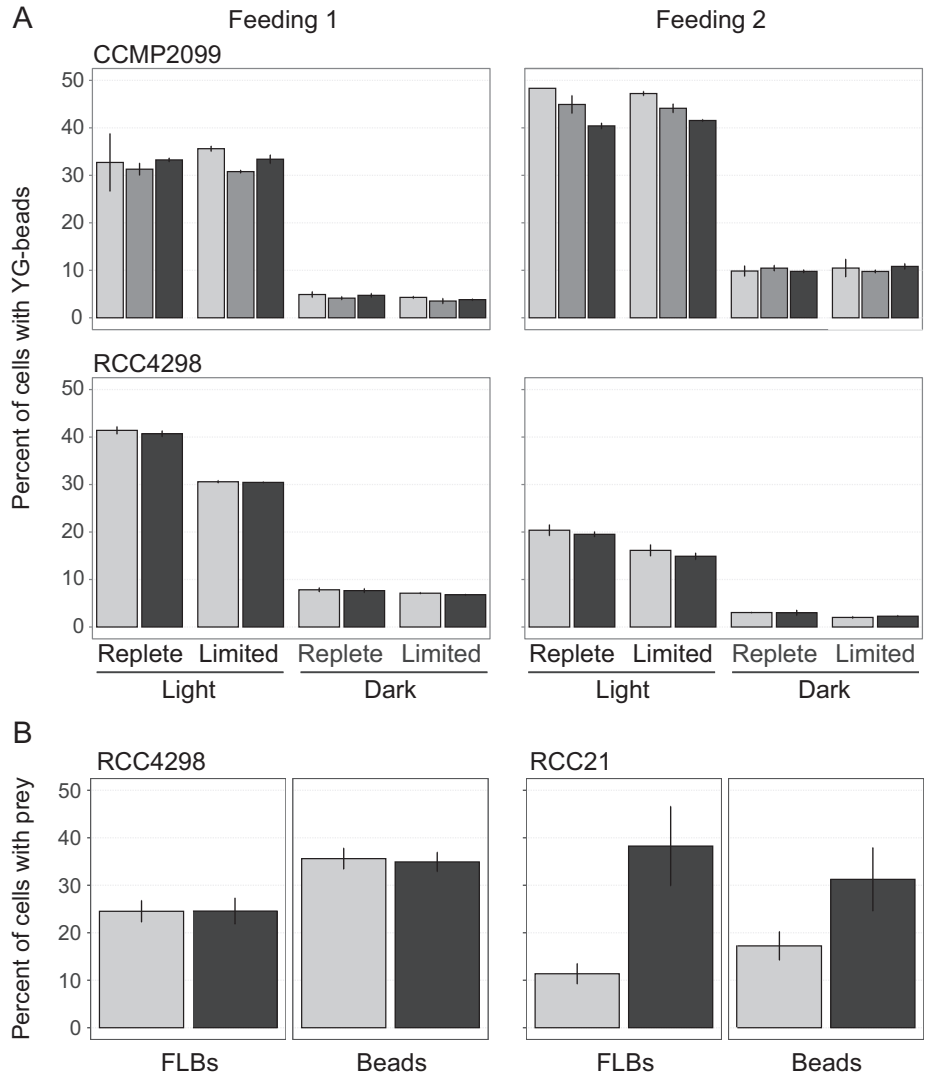

FIG. 2. (A) Percent of *Micromonas polaris* strains CCMP2009 and RCC4298 cells with YG-beads (*M. polaris*-EXP1) for different treatments. Two feeding experiments were performed. (B) Percent of *M. polaris* strain RCC4298 and *Ochromonas triangulata* strain RCC21 cells with FLBs and YG-beads (EXP3). The color of the bars corresponds to the time after the addition of YG-beads (0 min, light gray; 20 min, dark gray; 40 min, black). Error bars correspond to standard deviation.

light conditions. This contrasts with our data since we observed less attachment under dark conditions (Fig. 2A). However, in the Wilken et al. (2019) study cells were put in the dark for a maximum of 44 h (less than 2 d, their Fig. 3, a and b) while in our case we performed the first feeding experiment after 7 days (Fig. 1). Therefore, in our experiment the number of cells corresponding to our first feeding experiment was much higher in the light than in the dark (Fig. 1), and since we adjusted the bead concentration as a function of the cell concentration, the bead concentration was also much higher in the light vs. the dark condition. This explains why, based on Fig. 3 (linear relationship between % of cells with beads and bead concentration), we found a much higher % of cells with beads under the light condition. External attachment of particles or bacterial cells to phytoplankton cell surfaces may be enhanced by phycosphere properties (Bell and Mitchell 1972, Seymour et al. 2017) which mainly consist of polysaccharides released by the cells (Myklestad 1995, Passow 2002a, Muhlenbruch et al. 2018). The "stickiness" properties of abundant exopolysaccharides have mainly been studied in diatoms (Engel 2000, Passow 2002b, Seymour et al. 2017). Bacteria colonization of this sticky phycosphere occurs in both live and compromised cells and is a function of the probability of random encounters of phytoplankton and bacteria which is influenced by both bacteria concentration and motility (Seymour et al. 2017).

Our experimental conditions were very similar to those reported by McKie-Krisberg and Sanders (2014). We used the same *Micromonas polaris* strain

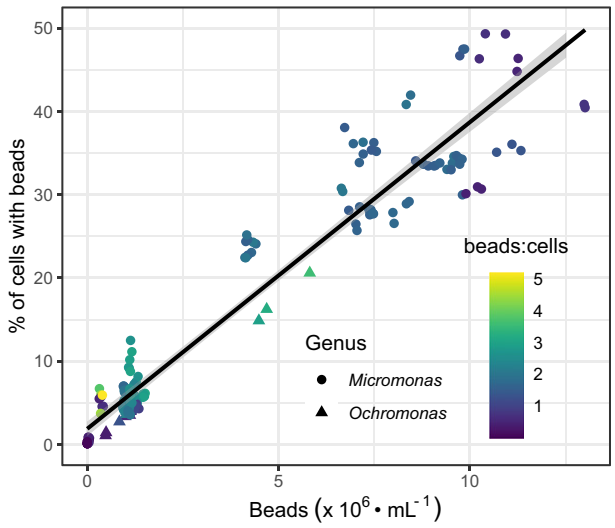

FIG. 3. Relationship between percent of cells with YG-beads and bead concentration immediately after the addition of YG-beads (T_0). The line and spread represent a fitted linear relationship ($R^2 = 0.93$). Circles correspond to *Micromonas polaris* and triangles to *Ochromonas triangulata* experiments. [Colour figure can be viewed at wileyonlinelibrary.com]

(CCMP2099), dark and light conditions, ASW for medium preparation, 0.5 µm beads, Lugol's iodine fixation, and short term incubation (40 min). The main methodological difference is that we used flow cytometry analysis of cell suspensions instead of epifluorescence microscopy of filtered samples. Our approach has many advantages over epifluorescence microscopy: it allows counting of a much larger number of cells (typically several thousand vs. 100-200); it is faster; it results in less potential biases related to individual operator interpretation; there is no ambiguity linked to food particles randomly overlapping with cells during filtration. The latter problem is demonstrated in McKie-Krisberg and Sanders (2014): Their differential interference contrast and confocal microscopy images (Fig. 1, c and d in their paper) aimed at demonstrating a YG-bead inside a *M. polaris* cell are inconclusive as the bead is at the edge of the cell (probably externally attached) which closely resembles the TEM images obtained in the present study (Fig. S8). The two other papers that have reported phago-mixotrophy in *Micromonas* (Gonzalez et al. 1993, Sanders and Gast 2012) may have suffered from the same problem, that is, initial attachment of prey to cells. Moreover, in the Sanders and Gast (2012) paper on natural communities the identity of the potential grazer was only "tentatively identified as *Micromonas*" from the presence of a DGGE band with a *Micromonas* sequence.

A study that examined gene expression of *M. polaris* strain CCMP2099 under nutrient stress conditions that could influence grazing rate failed to find differential expression of any gene linked to the process of phagocytosis in *M. polaris* (McKie-Krisberg et al. 2018). The authors propose that *M. polaris* may constitutively express phagocytosis proteins to support low-level grazing. However, a study on the model phagocyte *Dictyostelium discoideum* suggests that an increase in phagocytosis can indeed be linked to differential expression of genes involved in the process (Sillo et al. 2008). An alternative hypothesis regarding the gene expression results from *M. polaris*, supported by the data presented here, is that members of the genus *Micromonas* are not phagocytotic and therefore have no mechanism for differential expression of genes linked to phagocytosis. Sets of proteins identified as part of the phagosome compartment are broadly distributed among phagocyte and nonphagocyte organisms and only a small subset of those proteins are indicative that a species has the capacity for phagocytosis (Burns et al. 2018). Computational models show that members of the genus *Micromonas* lack those indicative proteins, reinforcing our hypothesis that *Micromonas* is not a phago-mixotroph.

It is now acknowledged that phago-mixotrophy is a widespread trait in planktonic communities and has profound implications for marine ecosystem functioning (Stoecker et al. 2017, Flynn et al. 2019). In particular, phago-mixotrophy is believed to provide a competitive advantage to photosynthetic organisms under otherwise limiting environmental conditions (e.g., low light, low nutrients). Bacterial phagocytosis has been found everywhere across the eukaryotic tree of life (Selosse et al. 2017), but most laboratory studies on phago-mixotrophy have focused on a few model organisms such as the chrysophyte *Ochromonas* spp. (e.g., Terrado et al. 2017, Lie et al. 2018, Wilken et al. 2020), the haptophytes *Prymnesium parvum* (e.g., Brutemark and Graneli 2011, Liu et al. 2015), and *Chrysochromulina* spp. (Jones et al. 1993, Hansen and Hjorth 2002), and several taxa of dinoflagellate such as *Alexandrium* spp. (e.g., Jeong et al. 2010, Hansen 2011, Lee et al. 2016). Among green algae in addition to the works on *Micromonas* mentioned previously, only a few studies have been performed with 6 other species described as phago-mixotrophs: *Pyramimonas gelicola* (Gast et al. 2014), *Pyramimonas tychotreta* and *Mantoniella antarctica* (McKie-Krisberg et al. 2015), *Cymbomonas tetramitiformis* (Maruyama and Kim 2013, Burns et al. 2015), *Nephroselmis rotunda* and *N. pyriformis* (Anderson et al. 2018). None of these species fall, however, in the picoplankton size range. Interestingly, none of the picoplanktonic Mamiellophyceae (in addition to *Micromonas*) for which the trait-based computational analysis was performed (*Bathycoccus*, *Ostreococcus*, *Mantoniella*, including *M. antarctica*) showed evidence for phago-mixotrophy. This may suggest that the whole Mamiellophyceae class (or at least the orders Mamiellales and Bathycoccales, since we have no data for orders Dolichomastigales and Monomastigales) does not contain phago-mixotrophic species. Despite being

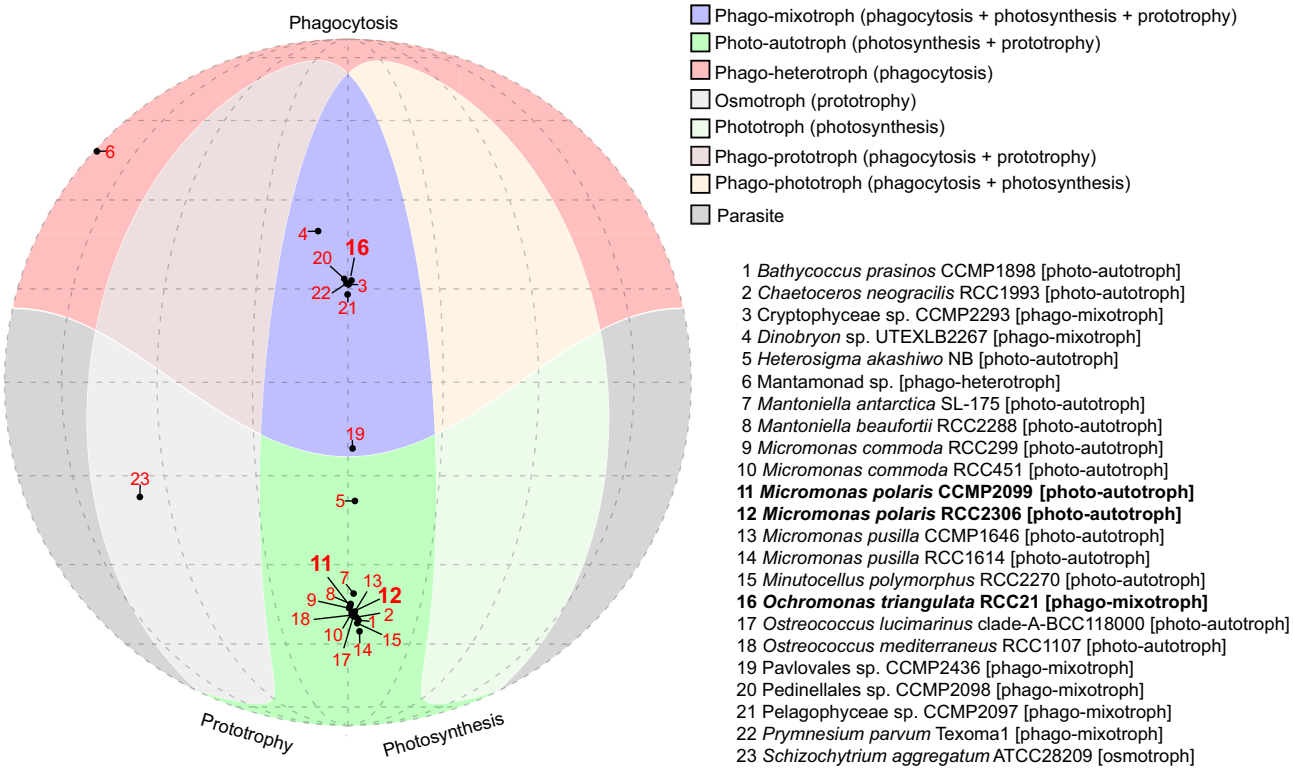

FIG. 4. Trophic mode predictions from genome and transcriptome analysis. Predictions in three dimensions, phagocytosis, photosynthesis, and prototrophy were projected onto the circle. Shaded regions indicate regions where 0 (parasite, gray, lower edges) to all 3 (phago-mixotroph, blue, upper central region) predictions cross the positive threshold of 50% probability of a strain possessing a given function. Organisms positive for phagotrophy are in the upper hemisphere. Organisms positive for photosynthesis are in the middle to right region. Organisms positive for prototrophy are in the middle to left region. Organisms negative for all predictions are in the lower gray edge regions. Strains in bold correspond to those used in the feeding experiments. [Colour figure can be viewed at wileyonline library.com]

primary players in many environments (Tragin and Vaulot 2018) including oligotrophic waters (Vannier et al. 2016), green picoeukaryotes are likely to rely on other strategies to thrive. Knowing the nutrition modes of this group will be important for modeling marine ecosystems since phago-mixotrophs increase the transfer of biomass to higher trophic levels resulting in larger organism mean size and sinking carbon fluxes (Ward and Follows 2016).

The evidence presented in this paper indicating that *Micromonas polaris* is unlikely to be a phago-mixotroph has profound impacts in present and future predictions of Arctic primary production, because of the importance and predicted increasing concentrations of this species in the Arctic Ocean (Li et al. 2009). If indeed *M. polaris* is not a phago-mixotroph, the question of how it survives during the long Arctic winter (Vader et al. 2015, Joli et al. 2017) and how it is able to develop during the Spring bloom that starts with very low light condition under the snow covered ice (Arrigo et al. 2012) remains open.

This paper is dedicated to the memory of Hervé Moreau, who was coordinating this research project and passed away too young in July 2020. This work was supported by ANR contract PhytoPol (ANR-15-CE02-0007). We thank Robert Sanders and Rebecca Gast for hosting VJ and training her on techniques to determine mixotrophy in phytoplankton. We also thank Dominique Marie for help with flow cytometry, Christian Jeanthon for help and advice with fluorescently labeled bacteria, Sophie Le Panse from the Merimage microscopy platform at the Roscoff Marine Station for assistance with the transmission electron micrographs and the Roscoff Culture Collection for providing of the algal strains.

AUTHOR CONTRIBUTIONS

DV and VJ conceived the study. VJ and FLG collected and processed the samples. VJ, JB, and DV analyzed the data. VJ, JB, and DV drafted the manuscript. VJ, DV, FLG, FN, and JB edited the final version of the paper.

Andersen, R. A., Graf, L., Malakhov, Y. & Yoon, H. S. 2017. Rediscovery of the *Ochromonas* type species *Ochromonas triangulata* (Chrysophyceae) from its type locality (Lake Veysove, Donetsk region, Ukraine). *Phycologia* 56:591–604.

Anderson, R., Charvet, S. & Hansen, P. J. 2018. Mixotrophy in Chlorophytes and Haptophytes: Effect of irradiance, macronutrient, micronutrient and vitamin limitation. *Front Microbiol.* 9:1704.

Arrigo, K. R., Perovich, D. K., Pickart, R. S., Brown, Z. W., Dijken, G. L. V., Lowry, K. E., Mills, M. M. et al. 2012. Massive phytoplankton blooms under Arctic Sea ice. *Science* 336:2012.

Arrigo, K. R., van Dijken, G. & Pabi, S. 2008. Impact of a shrinking Arctic ice cover on marine primary production. *Geophys. Res Let.* 35:297.

Balzano, S., Marie, D., Gourvil, P. & Vaulot, D. 2012. Composition of the summer photosynthetic pico and nanoplankton communities in the Beaufort Sea assessed by T-RFLP and sequences of the 18S rRNA gene from flow cytometry sorted samples. *ISME J.* 6:1480–98.

Bell, W. & Mitchell, R. 1972. Chemotactic and growth responses of marine bacteria to algal extracellular products. *Biol. Bull.* 143:265–77.

Benner, I., Irwin, A. J. & Finkel, Z. V. 2020. Capacity of the common Arctic picoeukaryote *Micromonas* to adapt to a warming ocean. *Limnol. Oceanogr. Lett.* 5:221–7.

Berge, J., Renaud, P. E., Darnis, G., Cottier, F., Last, K., Gabrielsen, T. M., Johnsen, G. et al. 2015. In the dark: A review of ecosystem processes during the Arctic polar night. *Prog. Oceanogr.* 139:258–71.

Box, J. E., Colgan, W. T., Christensen, T. R., Schmidt, N. M., Lund, M., Parmentier, F. J. W., Brown, R. et al. 2019. Key indicators of Arctic climate change: 1971–2017. *Environ. Res. Lett.* 14:045010.

Brown, N. J., Nilsson, J. & Pemberton, P. 2019. Arctic Ocean freshwater dynamics: Transient response to increasing river runoff and precipitation. *J. Geophys. Res. Oceans* 124:5205–19.

Brutemark, A. & Graneli, E. 2011. Role of mixotrophy and light for growth and survival of the toxic haptophyte *Prymnesium parvum*. *Harmful Algae* 10:388–94.

Burns, J. A., Paasch, A., Narechania, A. & Kim, E. 2015. Comparative genomics of a bacterivorous green alga reveals evolutionary causalities and consequences of phago-mixotrophic mode of nutrition. *Genome Biol. Evol.* 7:3047–61.

Burns, J. A., Pittis, A. A. & Kim, E. 2018. Gene-based predictive models of trophic modes suggest Asgard archaea are not phagocytotic. *Nat. Ecol. Evol.* 2:697–704.

Caron, D. A. 2016. Mixotrophy stirs up our understanding of marine food webs. *Proc. Natl. Acad. Sci. USA* 113:2806–8.

Carvalho, W. F. & Graneli, E. 2006. Acidotropic probes and flow cytometry: a powerful combination for detecting phagotrophy in mixotrophic and heterotrophic protists. *Aquat. Microb. Ecol.* 44:85–96.

Coupel, P., Ruiz-Pino, D., Sicre, M. A., Chen, J. F., Lee, S. H., Schiffrine, N., Li, H. L. & Gascard, J. C. 2015. The impact of freshening on phytoplankton production in the Pacific Arctic Ocean. *Prog. Oceanogr.* 131:113–25.

Engel, A. 2000. The role of transparent exopolymer particles (TEP) in the increase in apparent particle stickiness (α) during the decline of a diatom bloom. *J. Plankton Res.* 22:485–97.

Flynn, K. J., Mitra, A., Anestis, K., Anschutz, A. A., Calbet, A., Ferreira, G. D., Gypens, N. et al. 2019. Mixotrophic protists and a new paradigm for marine ecology: Where does plankton research go now? *J. Plankton Res.* 41:375–91.

Gast, R. J., McKie-Krisberg, Z. M., Fay, S. A., Rose, J. M. & Sanders, R. W. 2014. Antarctic mixotrophic protist abundances by microscopy and molecular methods. *FEMS Microbiol. Ecol.* 89:388–401.

Gonzalez, J. M., Sherr, B. & Sherr, E. B. 1993. Digestive enzyme activity as a quantitative measure of protistan grazing: the acid lysozyme assay for bacterivory. *Mar. Ecol. Prog. Ser.* 100:197–206.

Graversen, R. G., Mauritsen, T., Tjernström, M., Källén, E. & Svensson, G. 2008. Vertical structure of recent Arctic warming. *Nature* 451:53.

Guillard, R. R. L. & Hargraves, P. E. 1993. *Stichochrysis immobilis* is a diatom, not a chrysophyte. *Phycologia* 32:234–6.

Hansen, P. E. R. J. 2011. The role of photosynthesis and food uptake for the growth of marine mixotrophic dinoflagellates. *J. Eukaryot. Microbiol.* 58:203–14.

Hansen, P. J. & Hjorth, M. 2002. Growth and grazing responses of *Chrysochromulina ericina*. *Mar. Biol.* 141:975–83.

Hartmann, M., Grob, C., Tarran, G. A., Martin, A. P., Burkill, P. H., Scanlan, D. J. & Zubkov, M. V. 2012. Mixotrophic basis of Atlantic oligotrophic ecosystems. *Proc. Natl. Acad. Sci. USA* 109:5756–60.

Hoppe, C. J. M., Flintrop, C. M. & Rost, B. 2018. The Arctic picoeukaryote *Micromonas pusilla* benefits synergistically from warming and ocean acidification. *Biogeosciences* 15:4353–65.

Jeong, H. J., Yoo, Y. D., Kim, J. S., Seong, K. A., Kang, N. S. & Kim, T. H. 2010. Growth, feeding and ecological roles of the mixotrophic and heterotrophic dinoflagellates in marine planktonic food webs. *Ocean Sci. J.* 45:65–91.

Joli, N., Monier, A., Logares, R. & Lovejoy, C. 2017. Seasonal patterns in Arctic prasinophytes and inferred ecology of *Bathycoccus* unveiled in an Arctic winter metagenome. *ISME J.* 11:1372–85.

Jones, H. L. J., Leadbeater, B. S. C. & Green, J. C. 1993. Mixotrophy in marine species of *Chrysochromulina* (Prymnesiophyceae): ingestion and digestion of a small green flagellate. *J. Mar. Biolog.* 73:283–96.

Kahru, M., Lee, Z., Mitchell, B. G. & Nevison, C. D. 2016. Effects of sea ice cover on satellite detected primary production in the Arctic Ocean. *Biol. Lett.* 12:20160223.

Keeling, P. J., Burki, F., Wilcox, H. M., Allam, B., Allen, E. E., Amaral-Zettler, L. A., Armbrust, E. V. et al. 2014. The Marine Microbial Eukaryote Transcriptome Sequencing Project (MMETSP): Illuminating the functional diversity of eukaryotic life in the oceans through transcriptome sequencing. *PLoS Biol.* 12:e1001889.

Keller, M. D., Selvin, R. C., Claus, W. & Guillard, R. R. L. 1987. Media for the culture of oceanic ultraphytoplankton. *J. Phycol.* 23:633–8.

Kilias, E., Kattner, G., Wolf, C., Frickenhaus, S. & Metfies, K. 2014. A molecular survey of protist diversity through the central Arctic Ocean. *Polar Biol.* 37:1271–87.

Lee, K. H., Jeong, H. J., Kwon, J. E., Kang, H. C., Kim, J. H., Jang, S. H., Park, J. Y., Yoon, E. Y. & Kim, J. S. 2016. Mixotrophic ability of the phototrophic dinoflagellates *Alexandrium andersonii*, *A. affine*, and *A. fraterculus*. *Harmful Algae* 59:67–81.

Leles, S. G., Mitra, A., Flynn, K. J., Tillmann, U., Stoecker, D., Jeong, H. J., Burkholder, J. et al. 2019. Sampling bias misrepresents the biogeographical significance of constitutive mixotrophs across global oceans. *Glob. Ecol. Biogeogr.* 28:418–28.

Li, W. K., McLaughlin, F. A., Lovejoy, C. & Carmack, E. C. 2009. Smallest algae thrive as the Arctic Ocean freshens. *Science* 326:539.

Lie, A. A. Y., Liu, Z., Terrado, R., Tatters, A. O., Heidelberg, K. B. & Caron, D. A. 2018. A tale of two mixotrophic chrysophytes: Insights into the metabolisms of two *Ochromonas* species (Chrysophyceae) through a comparison of gene expression. *PLoS ONE* 13:e0192439.

Liu, Z., Koid, A. E., Terrado, R., Campbell, V., Caron, D. A. & Heidelberg, K. B. 2015. Changes in gene expression of *Prymnesium parvum* induced by nitrogen and phosphorus limitation. *Front. Microbiol.* 6:631.

Lovejoy, C., Vincent, W. F., Bonilla, S., Roy, S., Martineau, M. J., Terrado, R., Potvin, M., Massana, R. & Pedros-Alio, C. 2007. Distribution, phylogeny, and growth of cold-adapted picoprasinophytes in arctic seas. *J. Phycol.* 43:78–89.

Maia, R., Eliason, C. M., Bitton, P. P., Doucet, S. M. & Shawkey, M. D. 2013. Pavo: an R package for the analysis, visualization and organization of spectral data. *Methods Ecol. Evol.* 4:906–913.

Marquardt, M., Vader, A., Stubner, E. I., Reigstad, M. & Gabrielsen, T. M. 2016. Strong seasonality of marine microbial eukaryotes in a high-Arctic fjord (Isfjorden, in West Spitsbergen, Norway). *Appl. Environ. Microbiol.* 82:1868–80.

Maruyama, S. & Kim, E. 2013. A modern descendant of early green algal phagotrophs. *Curr. Biol.* 23:1081–4.

McKie-Krisberg, Z. M., Gast, R. J. & Sanders, R. W. 2015. Physiological responses of three species of Antarctic mixotrophic phytoflagellates to changes in light and dissolved nutrients. *Microb. Ecol.* 70:21–29.

McKie-Krisberg, Z. M. & Sanders, R. W. 2014. Phagotrophy by the picoeukaryotic green alga. *Micromonas*: implications for Arctic Oceans. *ISME J.* 10:1953–61.

McKie-Krisberg, Z. M., Sanders, R. W. & Gast, R. J. 2018. Evaluation of mixotrophy-associated gene expression in two species of polar marine algae. *Front. Mar. Sci.* 5:1–12.

Millette, N. C., Pierson, J. J., Aceves, A. & Stoecker, D. K. 2017. Mixotrophy in *Heterocapsa rotundata*: A mechanism for dominating the winter phytoplankton. *Limnol. Oceanogr.* 62:836–45.

Mitra, A., Flynn, K. J., Burkholder, J. M., Berge, T., Calbet, A., Raven, J. A., Graneli, E., Glibert, P. M., Hansen, P. J., Stoecker, D. K., Thingstad, F., Tillmann, U., Vage, S., Wilken, S. & Zubkov, M. V. 2014. The role of mixotrophic protists in the biological carbon pump. *Biogeosciences* 11:995–1005.

Muhlenbruch, M., Grossart, H.P., Eigemann, F. & Voss, M. 2018. Mini-review: Phytoplankton-derived polysaccharides in the marine environment and their interactions with heterotrophic bacteria. *Environ. Microbiol.* 20:2671–85.

Myklestad, S. M. 1995. Release of extracellular products by phytoplankton with special emphasis on polysaccharides. *Sci. Tot. Environ.* 165:155–64.

Nummelin, A., Ilicak, M., Li, C. & Smedsrud, L. H. 2016. Consequences of future increased. Arctic runoff on Arctic Ocean stratification, circulation, and sea ice cover. *J. Geophys. Res. Oceans* 121:617–37.

Park, J. Y., Kug, J. S., Bader, J., Rolph, R. & Kwon, M. 2015. Amplified Arctic warming by phytoplankton under greenhouse warming. *Proc. Natl. Acad. Sci. USA* 112:5921–6.

Passow, U. 2002a. Production of transparent exopolymer particles (TEP) by phyto- and bacterioplankton. *Mar. Ecol. Prog. Ser.* 236:1–12.

Passow, U. 2002b. Transparent exopolymer particles (TEP) in aquatic environments. *Prog. Oceanogr.* 55:287–333.

Paulsen, M. L., Dore, H., Garczarek, L., Seuthe, L., Muller, O., Sandaa, R. A., Bratbak, G. & Larsen, A. 2016. *Synechococcus* in the Atlantic Gateway to the Arctic Ocean. *Front. Mar. Sci.* 3:191.

R Core Team. 2014. *R: A Language and Environment for Statistical Computing*. R Foundation for Statistical Computing, Vienna, Austria.

Renaut, S., Devred, E. & Babin, M. 2018. Northward expansion and intensification of phytoplankton growth during the early ice-free season in Arctic. *Geophys. Res. Lett.* 45:10590–8.

Sanders, R. & Gast, R. 2012. Bacterivory by phototrophic picoplankton and nanoplankton in Arctic waters. *FEMS Microbiol. Ecol.* 82:242–53.

Selosse, M. A., Charpin, M. & Not, F. 2017. Mixotrophy everywhere on land and in water: the grand ecart hypothesis. *Ecol. Lett.* 20:246–63.

Seymour, J. R., Amin, S. A., Raina, J. B. & Stocker, R. 2017. Zooming in on the phyco-sphere: the ecological interface for phytoplankton–bacteria relationships. *Nat. Microbiol.* 2:17065.

Sherr, B. F., Sherr, E. B. & Fallon, R. D. 1987. Use of monodispersed, fluorescently labeled bacteria to estimate *in situ* protozoan bacterivory. *Appl. Environ. Microbiol.* 53:958–65.

Sherr, E. & Sherr, B. 1993. Protistan grazing rates via uptake of fluorescently labeled prey. *In* Kemp, P., Sherr, B., Sherr, E. & Cole, J. [Eds.] *Handbook of Methods in Aquatic Microbial Ecology*. Lewis Publishers, Boca Raton, FL, USA, pp. 695–701.

Sillo, A., Bloomfield, G., Balest, A., Balbo, A., Pergolizzi, B., Peracino, B., Skelton, J., Ivens, A. & Bozzaro, S. 2008. Genome-wide transcriptional changes induced by phagocytosis or growth on bacteria in *Dictyostelium*. *BMC Genom.* 9:291.

Simon, N., Foulon, E., Grulois, D., Six, C., Desdevises, Y., Latimier, M., Le Gall, F. et al. 2017. Revision of the genus *Micromonas* Manton et Parke (Chlorophyta, Mamiellophyceae), of the type species *M. pusilla* (Butcher) Manton & Parke and of the species *M. commoda* van Baren, Bachy and Worden and description of two new species based on the genetic and phenotypic characterization of cultured isolates. *Protist* 168:612–35.

Slagstad, D., Wassmann, P. F. J. & Ellingsen, I. 2015. Physical constrains and productivity in the future Arctic Ocean. *Front. Mar. Sci.* 2:1–23.

Stoecker, D. K., Hansen, P. J., Caron, D. A. & Mitra, A. 2017. Mixotrophy in the marine plankton. *Ann. Rev. Mar. Sci.* 9:311–35.

Stoecker, D. K. & Lavrentyev, P. J. 2018. Mixotrophic plankton in the polar seas: A pan-Arctic review. *Front. Mar. Sci.* 5:292.

Tedesco, L., Vichi, M. & Scoccimarro, E. 2019. Sea-ice algal phenology in a warmer Arctic. *Sci. Adv.* 5:eaav4830.

Terrado, R., Pasulka, A. L., Lie, A. A. Y., Orphan, V. J., Heidelberg, K. B. & Caron, D. A. 2017. Autotrophic and heterotrophic acquisition of carbon and nitrogen by a mixotrophic chrysophyte established through stable isotope analysis. *ISME J.* 11:2022.

Timmermans, M. L., Proshutinsky, A., Krishfield, R. A., Perovich, D. K., Richter-Menge, J. A., Stanton, T. P. & Toole, J. M. 2011. Surface freshening in the Arctic Ocean's Eurasian Basin: An apparent consequence of recent change in the wind-driven circulation. *J. Geophys. Res.* 116:C00D03.

Tragin, M. & Vaulot, D. 2018. Green microalgae in marine coastal waters: The Ocean Sampling Day (OSD) dataset. *Sci. Rep.* 8:14020.

Tremblay, J. E., Anderson, L. G., Matrai, P., Coupel, P., Bélanger, S., Michel, C. & Reigstad, M. 2015. Global and regional drivers of nutrient supply, primary production and CO_2 drawdown in the changing Arctic Ocean. *Prog. Oceanogr.* 139:171–96.

Unrein, F., Gasol, J. M., Not, F., Forn, I. & Massana, R. 2014. Mixotrophic haptophytes are key bacterial grazers in oligotrophic coastal waters. *ISME J.* 8:164–76.

Vader, A., Marquardt, M., Meshram, A. R. & Gabrielsen, T. M. 2015. Key Arctic phototrophs are widespread in the polar night. *Polar Biol.* 38:13–21.

van Baren, M. J., Bachy, C., Reistetter, E. N., Purvine, S. O., Grimwood, J., Sudek, S., Yu, H. et al. 2016. Evidence-based green algal genomics reveals marine diversity and ancestral characteristics of land plants. *BMC Genom.* 17:1–22.

Vannier, T., Leconte, J., Seeleuthner, Y., Mondy, S., Pelletier, E., Aury, J. M., de Vargas, C. et al. 2016. Survey of the green picoalga *Bathycoccus* genomes in the global ocean. *Sci. Rep.* 6:37900.

Ward, B. A. 2015. Temperature-correlated changes in phytoplankton community structure are restricted to polar waters. *PLoS ONE* 10:e0135581.

Ward, B. A. & Follows, M. J. 2016. Marine mixotrophy increases trophic transfer efficiency, mean organism size, and vertical carbon flux. *Proc. Natl. Acad. Sci. USA* 113:2958–63.

Wassmann, P. 2015. Overarching perspectives of contemporary and future ecosystems in the Arctic Ocean. *Prog. Oceanogr.* 139:1–12.

Wilken, S., Choi, C. J. & Worden, A. Z. 2020. Contrasting mixotrophic lifestyles reveal different ecological niches in two closely related marine protists. *J. Phycol.* 56:52–67.

Wilken, S., Yung, C. C. M., Hamilton, M., Hoadley, K., Nzongo, J., Eckmann, C., Corrochano-Luque, M., Poirier, C. & Worden, A. Z. 2019. The need to account for cell biology in characterizing predatory mixotrophs in aquatic environments. *Philos. Trans. R. Soc. Lond. B Biol. Sci.* 374:20190090.

Worden, A. Z., Lee, J. H., Mock, T., Rouze, P., Simmons, M. P., Aerts, A. L., Allen, A. E. et al. 2009. Green evolution and dynamic adaptations revealed by genomes of the marine picoeukaryotes *Micromonas*. *Science* 324:268–72.

Zhang, Q., Gradinger, R. & Spindler, M. 1998. Dark survival of marine microalgae in the high Arctic (Greenland Sea). *Polarforschung* 65:111–6.

Supporting Information

Additional Supporting Information may be found in the online version of this article at the publisher's web site:

Figure S1. Examples of flow cytograms for *Micromonas polaris* and the positive control *Ochromonas triangulata*. Examples of flow cytograms for *Micromonas polaris* and the positive control *Ochromonas triangulata*.

Figure S2. Flow cytograms of *Ochromonas triangulata* and *Micromonas polaris* before (purple) and after (green) staining with Lysosensor.

Figure S3. Change in forward scatter and red chlorophyll fluorescence measured by flow cytometry during the experiments reported in Figure 1 (*Micromonas polaris*-EXP1).

Figure S4. Percent of *Micromonas polaris* cells with YG-beads (*M. polaris*-EXP1) for strains RCC2258 and RCC2306 and different treatments.

Figure S5. Percent of *Micromonas polaris* cells with YG-beads (*M. polaris*-EXP2) for each strain and treatment.

Figure S6. Changes with time in the number of *Micromonas polaris* (strain RCC2306) cells with YG-beads measured by continuously running a live sample for 20 minutes immediately after the addition of YG-beads.

Figure S7. Flow cytograms for *Micromonas polaris* cells incubated with YG-beads of three different sizes: 0.5 (green), 1.0 (orange) and 2.0 (red) μm.

Figure S8. Transmission electron microscopy image of *Micromonas polaris* (strain RCC2306) with YG-beads (0.5 μm) after negative staining.

Table S1. List of strains used for transcriptome analysis.

Table S2. Summary of experimental conditions and results for all experiment performed with *Micromonas polaris* and *Ochromonas*.

Table S3. Comparison of feeding on three different YG-bead sizes (diameter 0.5, 1, and 2 μm) for *Micromonas polaris* (EXP7).

Table S4. Comparison of Lugol's iodine and glutaraldehyde fixation, and live (no fixation) measurements of the percent of *Micromonas polaris* cells with YG-beads (EXP6).

Table S5. Lysosensor experiment (EXP9). Last column shows the mean±sd of Lysosensor green fluorescence.